

Thermoelectric Properties of Iron- and Lanthanum-Doped CoSb₃ Compounds by Pulse Discharge Sintering

Takashi Itoh,* Eiji Hattori,[†] and Kuniyuki Kitagawa[‡]
Nagoya University, Nagoya 464-8603, Japan

DOI: 10.2514/1.22749

More than 60% of thermal energy generated through various combustion systems is discharged as waste heat into the atmosphere. Using the waste heat effectively is among the most important issues from a viewpoint of the depletion of fossil fuels. In this regard, thermoelectric power generation that can directly convert the thermal energy to electrical energy is one of the attractive methods. Skutterudite compounds of CoSb₃ have been investigated as promising candidate materials for thermoelectric power generation. In this research, CoSb₃ compounds were synthesized from raw metal powders by using a pulse discharge sintering process. To improve the thermoelectric properties, iron was doped as an element substituting for cobalt of the CoSb₃ compound. The syntheses of Fe_xCo_{1-x}Sb₃ were confirmed by x-ray diffraction analysis. The Seebeck coefficient, electric resistivity, and thermal conductivity were measured as the thermoelectric properties. Optimum content of iron was decided from the maximum thermoelectric figure of merit. Furthermore, filling of lanthanum into Fe_{0.1}Co_{0.9}Sb₃ was attempted to decrease the thermal conductivity. The lanthanum-filled Fe_{0.1}Co_{0.9}Sb₃ compounds were synthesized from raw metal powders and LaSb powder by the pulse discharge sintering process. The optimum lanthanum content that leads to the maximum thermoelectric performance is discussed. The substitution of iron for cobalt improved the thermoelectric performance. The lanthanum-filling decreased the thermal conductivity at a low lanthanum content and led to higher thermoelectric performance in spite of low lanthanum content.

Nomenclature

a	=	lattice constant, Å
L_0	=	Lorentz number, V ² K ⁻²
T	=	absolute temperature, K
x	=	iron content in Fe _x Co _{1-x} Sb ₃
x'	=	substituting iron content
y	=	lanthanum content in La _y Fe _{0.4} Co _{3.6} Sb ₁₂
Z	=	thermoelectric figure of merit, K ⁻¹
α	=	Seebeck coefficient, VK ⁻¹
θ	=	diffraction angle, deg
κ	=	thermal conductivity, W m ⁻¹ K ⁻¹
κ_E	=	electron thermal conductivity, W m ⁻¹ K ⁻¹
κ_L	=	lattice thermal conductivity, W m ⁻¹ K ⁻¹
λ	=	wavelength of the x-ray source, m
ρ	=	electrical resistivity, Ωm

I. Introduction

Thermal energy is generated through various combustion systems using combustion of fossil fuels such as petroleum, natural gas, and coal. However, more than 60% of thermal energy is discharged as waste heat into the atmosphere. From a viewpoint of saving energy, the effective use of the waste heat is a very important and urgent issue. Thermoelectric power generation that can directly convert thermal energy into electric energy is widely applicable to the power generation from milliwatts to megawatts in generating capacity. Thus, the thermoelectric power generation is a promising means using the waste heat discharged from energy systems such as

automobiles, combined cycles, and waste material incineration systems. Because conversion efficiency of thermoelectric power generation is still low, however, development of high-performance thermoelectric materials is indispensable for improvement of conversion efficiency and practical use.

In the thermoelectric research field, the dimensionless figure of merit ZT is frequently used as an index of thermoelectric performance [1]. This is defined as follows:

$$ZT \equiv \frac{\alpha^2 T}{\kappa \rho} \quad (1)$$

The product ZT is theoretically related with the conversion efficiency [1]. The higher ZT , the higher the conversion efficiency. The Seebeck coefficient α , the electrical resistivity ρ , and the thermal conductivity κ in Eq. (1) are the important three thermoelectric properties.

CoSb₃ skutterudite compounds are among the promising thermoelectric materials that are adequate for the thermoelectric power generation using heat resources with temperatures of 600 to 800 K. Uher [2] provided an in-depth review on skutterudite materials. The compounds have relatively good thermoelectric properties of the Seebeck coefficient and the electric conductivity. However, they do not demonstrate sufficient thermoelectric performance, because of a relatively high thermal conductivity. Lowering the thermal conductivity of skutterudite materials by phonon scattering is a very useful means to improve the thermoelectric performance [2]. Recently, the effect of fullerene addition to the thermoelectric properties has been reported on the skutterudite materials [3,4]. It was confirmed that dispersion of the fullerene particles in the skutterudite materials lowers the thermal conductivity by phonon scattering. Formation of solid solution is another approach to lower the thermal conductivity of skutterudite materials [5–7]. The most famous and major method of lowering the thermal conductivity of skutterudite materials is to fill atoms of rare-earth element into two voids (cages) existing in a unit cell of the skutterudite structure [2,8–13]. Figures 1a and 1b show the unit cells of the skutterudite structure and the filled skutterudite structure, respectively. The transition metal atoms form a simple cubic sublattice. The pnictogen atoms form planar quadrilateral rings that arrange along the (100), (010), or (001) crystallographic directions.

Received 26 January 2006; revision received 28 August 2007; accepted for publication 29 August 2007. Copyright © 2007 by the American Institute of Aeronautics and Astronautics, Inc. All rights reserved. Copies of this paper may be made for personal or internal use, on condition that the copier pay the \$10.00 per-copy fee to the Copyright Clearance Center, Inc., 222 Rosewood Drive, Danvers, MA 01923; include the code 0748-4658/08 \$10.00 in correspondence with the CCC.

*Associate Professor, Division of Integrated Research Projects, EcoTopia Science Institute, Furo-cho, Chikusa-ku.

[†]Graduate Student, Department of Applied Chemistry, Graduate School of Engineering, EcoTopia Science Institute, Furo-cho, Chikusa-ku

[‡]Professor, Division of Energy Science, EcoTopia Science Institute, Furo-cho, Chikusa-ku. Member AIAA.

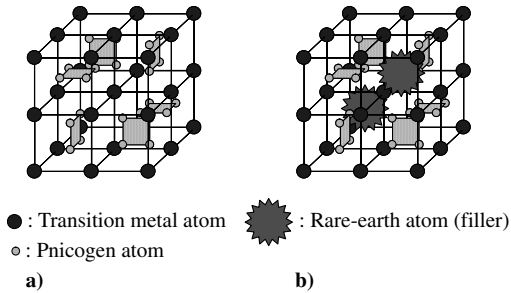


Fig. 1 Unit cells of a) skutterudite structure and b) filled skutterudite structure.

The unit cell has six such pnictogen rings. Two of the eight small cubes do not have the pnictogen ring, giving rise to two voids per unit cell of skutterudite structure (see Fig. 1a). In the crystal structure of the filled skutterudite, the rare-earth atoms occupy the two voids as filler atoms, as shown in Fig. 1b. The filler atoms have the thermal oscillation (rattling) during thermal transfer through the crystal lattice. This phenomenon brings about phonon scattering and consequently lowers the thermal conductivity.

In this research, the CoSb_3 compounds doped with iron and lanthanum were investigated to lower the thermal conductivity and to improve the thermoelectric performance. The iron element was doped for formation of solid solution, and the lanthanum element was doped for filling voids in the skutterudite structure. Pulse discharge sintering (PDS) is a type of hot-pressing method, which has an advantage of rapid and active sintering at relatively low temperatures. The PDS process is also effective for quick synthesis of the CoSb_3 compound [4]. Thus, the PDS process was used for synthesis of Fe-doped CoSb_3 compounds in place of the conventional melting method [13,14]. The syntheses of $\text{Fe}_x\text{Co}_{1-x}\text{Sb}_3$ were confirmed by x-ray diffraction (XRD) analysis. The thermoelectric properties (that is, Seebeck coefficient, electric resistivity, and thermal conductivity) were measured and an optimum iron content was decided from the maximum dimensionless figure of merit. Furthermore, filling lanthanum into $\text{Fe}_{0.1}\text{Co}_{0.9}\text{Sb}_3$ was attempted to achieve lower thermal conductivity. The PDS process was also used for synthesis of La-filled $\text{Fe}_{0.1}\text{Co}_{0.9}\text{Sb}_3$ compounds. The optimum La content that leads to the maximum thermoelectric performance is discussed.

II. Experimental

The commercial cobalt powder (purity of 99% or more and size of 75 μm or less), iron powder (99.9% or more and size of 5–6 μm), antimony powder (99.9% or more and size of 45 μm or less) were blended in a nonstoichiometric mole ratio of $\text{Fe}_x\text{Co}_{1-x}\text{Sb}_3$ ($x = 0, 0.04, 0.08, 0.1, 0.2, 0.3, 0.4$). The resulting powder mixture was sintered by PDS (SPS-1050, SPS Syntex Inc.). In the PDS process, on-off dc pulse voltage and current are repeatedly applied to the powder materials under compressive condition, and the powder with the surface activated by spark discharge is easily consolidated by Joule heating. After packing the powder into a graphite container, disk-type sintered samples ($\phi 20 \times 4$ mm) were prepared under the sintering conditions of compression at 60 MPa, a sintering temperature of 853 K, a holding time of 10 min, and a cooling speed of 2 K/min in a vacuum. On the other hand, the LaSb powder (purity of 99.9% or more and size of 300 μm or less) was newly added into the separately prepared powder mixtures of Co, Fe, and Sb to synthesize the $\text{La}_y\text{Fe}_{0.4}\text{Co}_{3.6}\text{Sb}_{12}$ compound ($y = 0.05, 0.1, 0.15, 0.4$) and the blended mixtures were sintered under the same sintering conditions. Density of the sintered sample was calculated from the volume and weight of the sample. The phases synthesized after PDS were identified and lattice constants were estimated by XRD analysis with $\text{Cu K}\alpha$ radiation (RINT2500TTR, Rigaku Corp.). The lattice constant in the skutterudite structure was calculated from the x-ray diffraction peaks of skutterudite in the diffraction angle 2θ range from 20 to 140 deg.

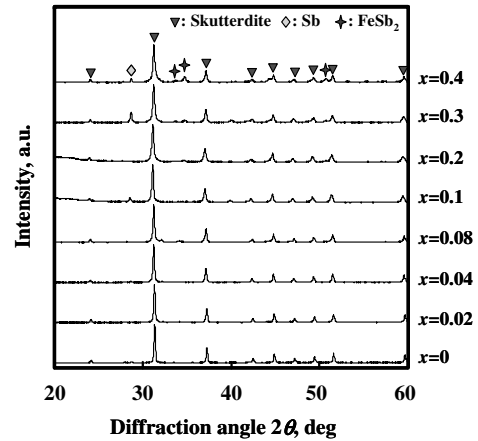


Fig. 2 X-ray diffraction patterns of $\text{Fe}_x\text{Co}_{1-x}\text{Sb}_3$ samples with various Fe contents.

After the sintered samples were cut into the prescribed shape, their Seebeck coefficient and electrical resistivity were measured with thermoelectric measuring equipment (ZEM-2, ULVAC-RIKO, Inc.), based on steady direct current and direct current four-terminal methods, respectively. The thermal conductivity was estimated with thermal constants measuring equipment (TC-7000, ULVAC-RIKO, Inc.), based on the laser-flash method.

III. Results and Discussion

Fe-doped CoSb_3 compounds were synthesized by the PDS process to lower the thermal conductivity by the effect of solid solution. Structural characteristics and thermoelectric properties of the compounds were investigated for determining an optimum Fe content at which the maximum thermoelectric performance is obtained. La-doped $\text{Fe}_{0.1}\text{Co}_{0.9}\text{Sb}_3$ compounds were also prepared by the PDS process to further lower the thermoelectric conductivity by effects of La filling. An optimum La content was determined from structural characteristics and thermoelectric properties of the compounds.

A. Structural Characteristics and Thermoelectric Properties of $\text{Fe}_x\text{Co}_{1-x}\text{Sb}_3$ Samples

All of the $\text{Fe}_x\text{Co}_{1-x}\text{Sb}_3$ samples prepared by the PDS process had a relative density of more than 95% regardless of Fe contents. Figure 2 shows the x-ray diffraction patterns of $\text{Fe}_x\text{Co}_{1-x}\text{Sb}_3$ samples prepared at various Fe contents. In the Fe content range from 0 to 0.08, only a single phase of skutterudite was identified. It is thought that Fe atoms substituted sufficiently for Co sites in the CoSb_3 structure, because other phases containing iron element were not detected. At an Fe content higher than 0.10, a diffraction peak of the FeSb_2 compound existed around 35 deg and the intensity of this peak increased with increasing Fe content. At an Fe content of 0.30 and 0.40, the Sb phase (see the peak of 28.7 deg in Fig. 2) existed together with the skutterudite phase and the FeSb_2 phase. Peng et al. [6] reported a similar result: that Sb and FeSb_2 phases exist at an Fe content higher than 0.16. These results would indicate that there is a threshold Fe content at which Sb and FeSb_2 phases begin to appear.

To confirm the substitution of Fe atoms for Co sites, the lattice constant of the skutterudite structure was calculated from the x-ray diffraction peaks of skutterudite. Figure 3 shows a change in the lattice constant with the Fe content. The lattice constant monotonously increased with the Fe content. This indicates that the unit cell of the skutterudite was expanded by substituting the iron atoms for a part of the cobalt sites. A relation based on Vegard's law that there is a linear relation between the lattice constant and the content of constituent atom in the solid solution is expressed as a broken line in Fig. 3. The change in the lattice constant deviated from the broken line at an Fe content higher than 0.04. The difference between nominal Fe content x and substituting Fe content x'

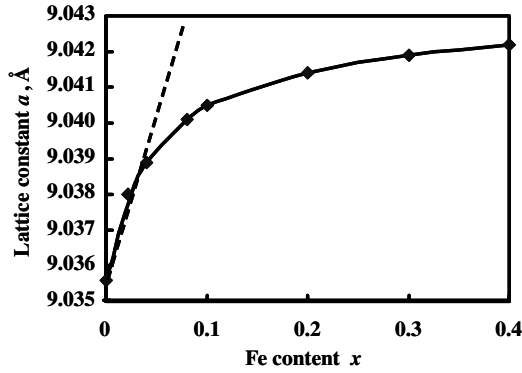
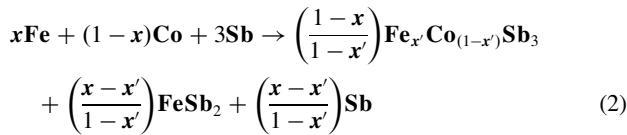


Fig. 3 Relation between Fe content x and the lattice constant of skutterudite in $\text{Fe}_x\text{Co}_{1-x}\text{Sb}_3$ samples; a broken line shows linear relation based on Vegard's law.

calculated from the lattice constant based on Vegard's law corresponds to an excess content of Fe. The existence of Fe atoms that cannot substitute for Co sites of CoSb_3 would result in the formations of the FeSb_2 phase and incidental Sb phase according to the following chemical reaction:



The amount of FeSb_2 and Sb phases would increase with an excess content of Fe. Though Fig. 3 suggests that FeSb_2 and Sb phases exist at an Fe content higher than 0.04, it is different from the result obtained by XRD analysis. These phases might not be detected at Fe contents of 0.08 and 0.1 due to the small amount of their phases.

Temperature dependence of the electrical resistivity in $\text{Fe}_x\text{Co}_{1-x}\text{Sb}_3$ samples is shown in Fig. 4. Only the CoSb_3 sample indicates negative temperature dependence. On the other hand, all samples of $\text{Fe}_x\text{Co}_{1-x}\text{Sb}_3$ ($0 < x \leq 0.4$) indicate positive temperature dependence and maintain the low level of electrical resistivity. The electrical resistivity drastically decreased by Fe doping in the lower temperature range. In the Fe content range from 0.04 to 0.2, the changes in electrical resistivity were almost the same. At an Fe content higher than 0.2, the electrical resistivity decreased with increasing Fe content.

Figure 5 shows measurement results of the Seebeck coefficient in $\text{Fe}_x\text{Co}_{1-x}\text{Sb}_3$ samples. Changes in the Seebeck coefficient of $\text{Fe}_x\text{Co}_{1-x}\text{Sb}_3$ samples were very different from that of the CoSb_3 sample. Fe doping lowered the Seebeck coefficient in the lower temperature range and it increased the peak temperature at which the peak of the Seebeck coefficient was obtained. In the Fe content range from 0.04 to 0.2, the Seebeck coefficient increased with the Fe content. At an Fe content higher than 0.2, it decreased with increasing Fe content.

The results of thermal conductivity in $\text{Fe}_x\text{Co}_{1-x}\text{Sb}_3$ samples are shown in Fig. 6. In the Fe content range from 0 to 0.1, the thermal conductivity decreased with increasing Fe content. This would be caused by substituting Fe for the Co site in the skutterudite structure. The samples with an Fe content higher than 0.2 had different temperature dependence of the thermal conductivity. It is thought that the cause would be due to the existence of the Sb and FeSb_2 phases. Temperature dependence of the thermal conductivity in the sample with an Fe content of 0.2 was in a transitional state. The formation of the Sb phase having high thermal conductivity would increase the thermal conductivity, and the increase in the amount of FeSb_2 phase would lower the thermal conductivity.

Figure 7 shows the results of the dimensionless figure of merit in the $\text{Fe}_x\text{Co}_{1-x}\text{Sb}_3$ samples. Fe doping increased the peak temperature at which the peak value of the dimensionless figure of merit ZT is obtained. The peak temperatures of the samples with different Fe contents were almost the same value of about 700 K. The maximum

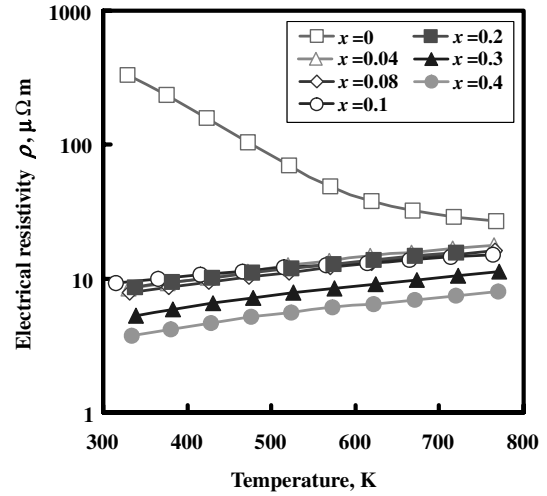


Fig. 4 Temperature dependence of electrical resistivity in $\text{Fe}_x\text{Co}_{1-x}\text{Sb}_3$ samples.

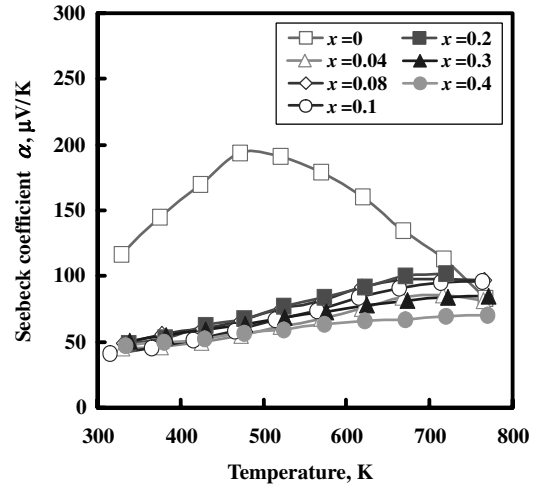


Fig. 5 Temperature dependence of the Seebeck coefficient in $\text{Fe}_x\text{Co}_{1-x}\text{Sb}_3$ samples.

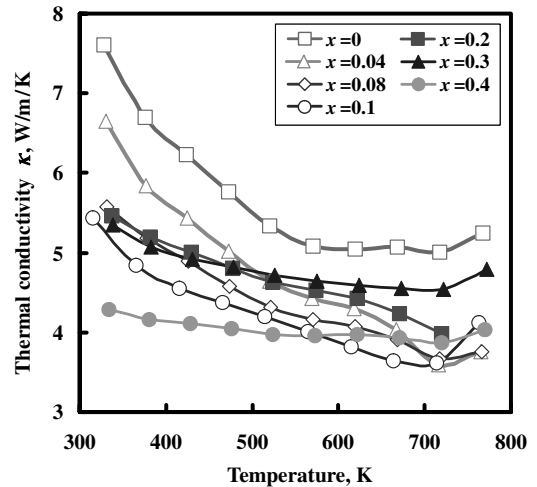


Fig. 6 Temperature dependence of thermal conductivity in $\text{Fe}_x\text{Co}_{1-x}\text{Sb}_3$ samples.

ZT of 0.12 at 723 K was obtained in the $\text{Fe}_{0.1}\text{Co}_{0.9}\text{Sb}_3$ sample ($x = 0.1$). The $\text{Fe}_{0.1}\text{Co}_{0.9}\text{Sb}_3$ sample was selected as a material with optimum Fe content from the standpoint of maximum thermoelectric performance. Filling La atoms into voids in a unit cell of the

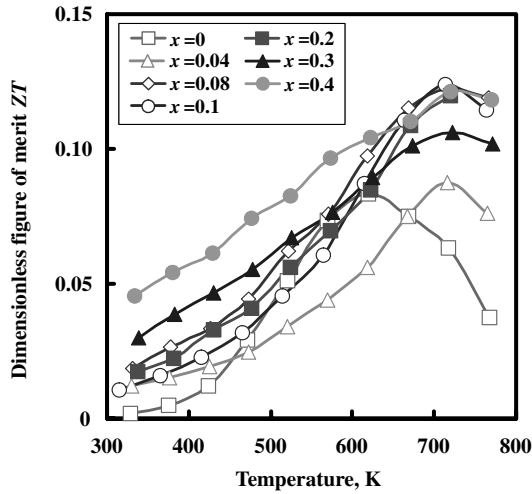


Fig. 7 Temperature dependence of the dimensionless figure of merit in $\text{Fe}_x\text{Co}_{1-x}\text{Sb}_3$ samples.

$\text{Fe}_{0.1}\text{Co}_{0.9}\text{Sb}_3$ sample was attempted as a next step. The samples were prepared by the PDS process and the structural characteristics and the thermoelectric properties were investigated to find an optimum La content for La filling.

B. Structural Characteristics and Thermoelectric Properties of $\text{La}_y\text{Fe}_{0.44}\text{Co}_{3.6}\text{Sb}_{12}$ Samples

To investigate the effect of La doping on the synthesized phase, an XRD analysis was carried out. Figure 8 shows the x-ray diffraction patterns of $\text{La}_y\text{Fe}_{0.44}\text{Co}_{3.6}\text{Sb}_{12}$ samples prepared at various La contents. Only a skutterudite phase was identified at any La content. The residual phases of LaSb and La were not detected from XRD analysis. Figure 9 shows the influence of the La content on the lattice constant in $\text{La}_y\text{Fe}_{0.44}\text{Co}_{3.6}\text{Sb}_{12}$ samples. A broken line in this figure expresses the average lattice constant of 9.0408 Å. There was no significant change in the lattice constant. This suggests that the La atoms would be inserted into voids in the unit cell of the skutterudite structure as filler atoms and they would hardly influence on the framework of the unit cell. All of the $\text{La}_y\text{Fe}_{0.44}\text{Co}_{3.6}\text{Sb}_{12}$ samples prepared by the PDS process also had a relative density of more than 95% regardless of the La contents.

The thermoelectric properties measured are shown in Figs. 10–12, respectively. Figure 10 shows the temperature dependence of the electrical resistivity in $\text{La}_y\text{Fe}_{0.44}\text{Co}_{3.6}\text{Sb}_{12}$ samples. Although there were linear relations between the electrical resistivity and the temperature in all the samples, the slope in the $\text{Fe}_{0.1}\text{Co}_{0.9}\text{Sb}_3$ sample ($y = 0$) was different from those in $\text{La}_y\text{Fe}_{0.44}\text{Co}_{3.6}\text{Sb}_{12}$ samples. The electrical resistivity slightly decreased with increasing La content.

Figure 11 shows the measurement results of the Seebeck coefficient in $\text{La}_y\text{Fe}_{0.44}\text{Co}_{3.6}\text{Sb}_{12}$ samples. The temperature dependence of the Seebeck coefficient in all samples had a similar tendency. Though Seebeck coefficients of $\text{La}_y\text{Fe}_{0.44}\text{Co}_{3.6}\text{Sb}_{12}$ samples were higher than that of the $\text{Fe}_{0.1}\text{Co}_{0.9}\text{Sb}_3$ sample ($y = 0$), it slightly decreased with increasing La content.

Temperature dependence of the thermal conductivity in $\text{La}_y\text{Fe}_{0.44}\text{Co}_{3.6}\text{Sb}_{12}$ samples with various La contents are shown in Fig. 12. The temperature dependence of the thermal conductivity in all samples indicated a similar tendency. The thermal conductivity was minimized at an La content of 0.05 over the range of all measurement temperatures. At an La content higher than 0.05, the thermal conductivity slightly increased with La content.

The thermal conductivity of thermoelectric materials is generally expressed as a total of the thermal conductivities due to the lattice and electronic contributions as follows:

$$\kappa = \kappa_L + \kappa_E \quad (3)$$

According to the Wiedemann–Franz Law, the electron thermal conductivity κ_E is expressed as follows:

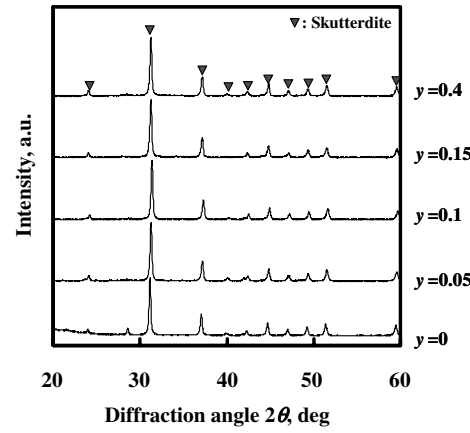


Fig. 8 X-ray diffraction patterns of $\text{La}_y\text{Fe}_{0.44}\text{Co}_{3.6}\text{Sb}_{12}$ samples with various La contents.

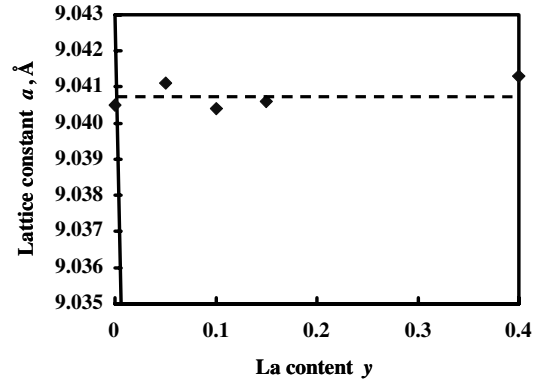


Fig. 9 Influence of La content on the lattice constant of $\text{La}_y\text{Fe}_{0.44}\text{Co}_{3.6}\text{Sb}_{12}$ samples; a broken line indicates average value.

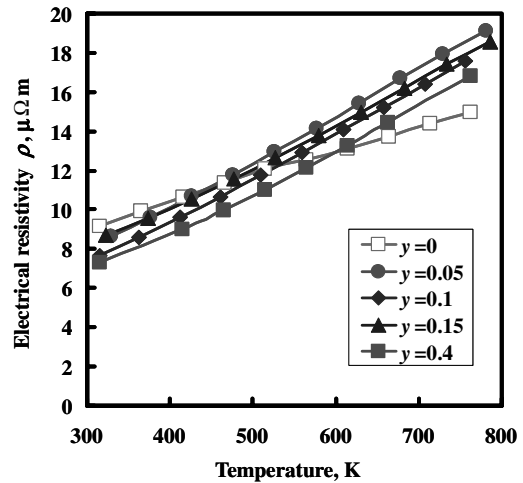


Fig. 10 Temperature dependence of electrical resistivity in $\text{La}_y\text{Fe}_{0.44}\text{Co}_{3.6}\text{Sb}_{12}$ samples.

$$\kappa_E = \frac{L_0 T}{\rho} \quad (4)$$

where the Lorentz number L_0 is $2.45 \times 10^{-8} \text{ V}^2 \text{ K}^{-2}$. The lattice thermal conductivity κ_L is estimated as the difference between the total thermal conductivity and the electron thermal conductivity.

Figure 13 shows the changes in the two types of thermal conductivities calculated using Eqs. (3) and (4). The electron thermal conductivity was much lower than the lattice thermal conductivity in

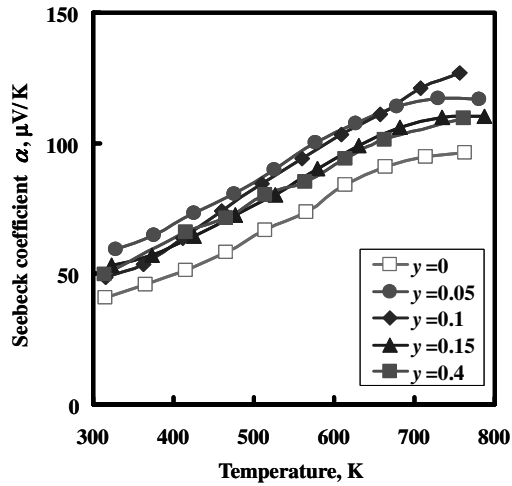


Fig. 11 Temperature dependence of the Seebeck coefficient in $\text{La}_y\text{Fe}_{0.4}\text{Co}_{3.6}\text{Sb}_{12}$ samples.

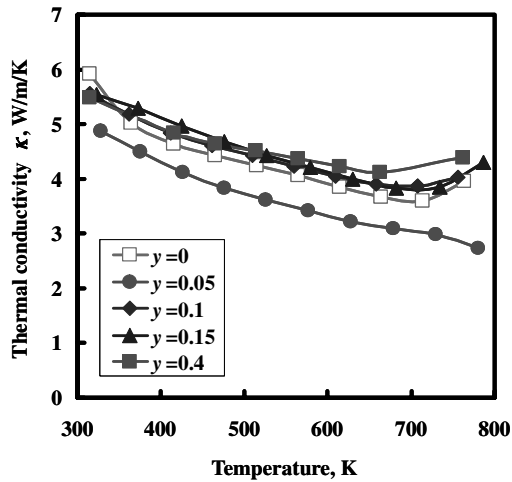
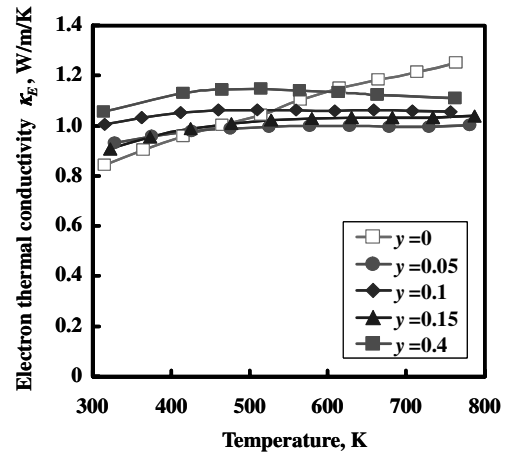


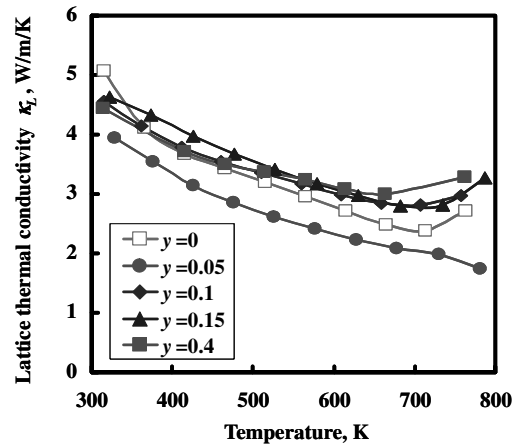
Fig. 12 Temperature dependence of thermal conductivity in $\text{La}_y\text{Fe}_{0.4}\text{Co}_{3.6}\text{Sb}_{12}$ samples.

all $\text{La}_y\text{Fe}_{0.4}\text{Co}_{3.6}\text{Sb}_{12}$ samples. The temperature dependence of the electron thermal conductivity in the La-doped samples indicated a different tendency from that in $\text{Fe}_{0.1}\text{Co}_{0.9}\text{Sb}_3$ samples. The electron thermal conductivity of the $\text{La}_y\text{Fe}_{0.4}\text{Co}_{3.6}\text{Sb}_{12}$ sample had a tendency of increasing with La content. The lattice thermal conductivity of the $\text{La}_y\text{Fe}_{0.4}\text{Co}_{3.6}\text{Sb}_{12}$ sample was minimized at an La content of 0.05, as well as the total thermal conductivity. Phonon scattering occurring by rattling of La atoms inserted into voids in the skutterudite structure would contribute to lowering of the lattice thermal conductivity. Excess La content ($y > 0.05$) increased the lattice thermal conductivity. Though La and LaSb phases were not detected in XRD analysis, existence of their phases having high thermal conductivity might increase the lattice thermal conductivity.

Figure 14 shows the temperature dependence of the dimensionless figure of merit ZT in $\text{La}_y\text{Fe}_{0.4}\text{Co}_{3.6}\text{Sb}_{12}$ samples together with that in the CoSb_3 sample. A peak of ZT in the $\text{La}_y\text{Fe}_{0.4}\text{Co}_{3.6}\text{Sb}_{12}$ sample existed at a higher temperature compared with that of the CoSb_3 sample, and the peak value of ZT was increased by doping Fe and La. Doping Fe and La would bring about phonon scattering according to effects of both the solid solution and the rattling of filler atoms and contribute to lowering of the thermal conductivity and to improvement of the thermoelectric performance. The maximum ZT of 0.20 at 781 K was obtained in the $\text{La}_y\text{Fe}_{0.4}\text{Co}_{3.6}\text{Sb}_{12}$ sample with an optimum La content of 0.05. The value was 2.4 times higher than that of the CoSb_3 sample. The optimum La content in this study is thought to correspond to the effective La-filling content in the $\text{La}_y\text{Fe}_{0.4}\text{Co}_{3.6}\text{Sb}_{12}$ sample. Because the effective La-filling content



a)



b)

Fig. 13 Temperature dependence of two types of thermal conductivities in $\text{La}_y\text{Fe}_{0.4}\text{Co}_{3.6}\text{Sb}_{12}$ samples: a) electron thermal conductivity and b) lattice thermal conductivity.

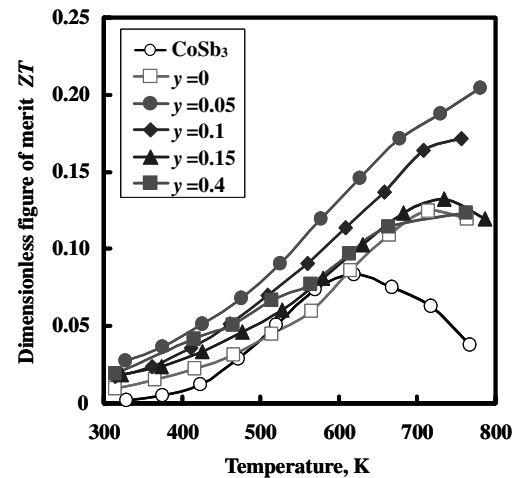


Fig. 14 Temperature dependence of the dimensionless figure of merit in $\text{La}_y\text{Fe}_{0.4}\text{Co}_{3.6}\text{Sb}_{12}$ samples.

of 0.05 is still low, the further improvement of thermoelectric performance (that is, $ZT > 1$) could be achieved by investigation of optimum content of both Fe and La for raising the effective La-filling content. In the operating conditions of PDS process, the sintering temperature, pressure, and holding time were fixed in this research. It would be necessary to optimize these operating conditions for achieving better thermoelectric performance of the filled skutterudite compounds.

IV. Conclusions

In this research, Fe- and La-doped CoSb_3 compounds were synthesized from raw metal powders by using a pulse discharge sintering (PDS) process. The structural features and the thermoelectric properties of the compounds were investigated. To lower the thermal conductivity by formation of solid solution and to improve the thermoelectric performance, $\text{Fe}_x\text{Co}_{1-x}\text{Sb}_3$ samples were prepared using a PDS process. The syntheses of $\text{Fe}_x\text{Co}_{1-x}\text{Sb}_3$ skutterudite compounds were confirmed by XRD analysis. The upper limit of the Fe content, in which a single phase of the $\text{Fe}_x\text{Co}_{1-x}\text{Sb}_3$ compound exists, was 0.08. The lattice constant of skutterudite was monotonously increased with the Fe content. The electrical resistivity and the Seebeck coefficient dropped extremely at relatively low temperature by doping a small amount of Fe. The thermal conductivity also decreased with increase of the Fe content. The maximum dimensionless figure of merit of 0.12 at 723 K was obtained in the $\text{Fe}_{0.1}\text{Co}_{0.9}\text{Sb}_3$ sample ($x = 0.1$) and exceeded that of CoSb_3 ($ZT = 0.08$). An optimum Fe content in the $\text{Fe}_x\text{Co}_{1-x}\text{Sb}_3$ sample was decided as the $x = 0.1$ form standpoint of maximizing thermoelectric performance. To lower the thermal conductivity by La filling and to improve the thermoelectric performance, $\text{La}_y\text{Fe}_{0.4}\text{Co}_{3.6}\text{Sb}_{12}$ samples were prepared using a PDS process. A single phase of skutterudite compound was only detected in all $\text{La}_y\text{Fe}_{0.4}\text{Co}_{3.6}\text{Sb}_{12}$ samples. An effective La-filling content was estimated as 0.05, because the $\text{La}_{0.05}\text{Fe}_{0.4}\text{Co}_{3.6}\text{Sb}_{12}$ sample had the minimum lattice thermal conductivity at the Fe content. The maximum figure of merit of 0.20 at 781 K was obtained in the $\text{La}_{0.05}\text{Fe}_{0.4}\text{Co}_{3.6}\text{Sb}_{12}$ sample and exceeded the performances of CoSb_3 and $\text{Fe}_{0.10}\text{Co}_{0.90}\text{Sb}_3$. The maximum value was 2.4 times that of the CoSb_3 sample. Further improvement of thermoelectric performance (that is, $ZT > 1$) could be achieved by investigation of the optimum content of both Fe and La for raising the effective La-filling content.

Acknowledgment

This work was supported by a Grant-in-Aid for Scientific Researches by the Ministry of Education, Culture, Sports, Science and Technology of the Government of Japan.

References

- [1] Goldsmid, H. J., "Introduction," *Semiconductors and Semimetals*, edited by T. M. Tritt, Vol. 69, Academic Press, San Diego, CA, 2001, pp. 1–24.
- [2] C. Uher, "Skutterudites: Prospective Novel Thermoelectrics," *Semiconductors and Semimetals*, edited by T. M. Tritt, Vol. 69, Academic Press, San Diego, CA, 2001, pp. 139–253.
- [3] Shi, X., Chen, L., Yang, J., and Meisner, G. P., "Enhanced Thermoelectric Figure of Merit of CoSb_3 via Large-Defect Scattering," *Applied Physics Letters*, Vol. 84, No. 13, 2004, pp. 2301–2303. doi:10.1063/1.1687997
- [4] Itoh, T., Ishikawa, K., and Okada, A., "Effect Of Fullerene Addition on Thermoelectric Properties of N-Type Skutterudite Compound," *Journal of Materials Research*, Vol. 22, No. 1, 2007, pp. 249–253. doi:10.1557/jmr.2007.0031
- [5] Katsuyama, S., Shichijo, Y., Ito, M., Majima, K., and Nagai, H., "Thermoelectric Properties of the Skutterudite $\text{Co}_{1-x}\text{Fe}_x\text{Sb}_3$ System," *Journal of Applied Physics*, Vol. 84, No. 12, 1998, pp. 6708–6712. doi:10.1063/1.369048
- [6] Peng, J., Yang, J., Song, X., Chen, Y., and Zhang, T., "Effect of Fe Substitution on the Thermoelectric Transport Properties of CoSb_3 -Based Skutterudite Compound," *Journal of Alloys and Compounds*, Vol. 426, Nos. 1–2, 2006, pp. 7–11. doi:10.1016/j.jallcom.2006.02.003
- [7] Ur, S.-C., Kwon, J.-C., and Kim, I.-H., "Thermoelectric Properties of Fe-Doped CoSb_3 Prepared by Mechanical Alloying and Vacuum Hot Pressing," *Journal of Alloys and Compounds*, Vol. 442, Nos. 1–2, 2007, pp. 358–361. doi:10.1016/j.jallcom.2006.08.369
- [8] Nolas, G. S., Kaeser, M., Littleton, R. T., IV, and Tritt, T. M., "High Figure of Merit in Partially Filled Ytterbium Skutterudite Materials," *Applied Physics Letters*, Vol. 77, No. 12, 2000, pp. 1855–1857. doi:10.1063/1.1311597
- [9] Anno, H., Ashida, K., Matsubara, K., Nolas, G. S., Akai, K., Matsuura, M., and Nagao, J., "Electronic Structure and Thermoelectric Properties of Ytterbium-Filled Skutterudites," *Thermoelectric Materials 2001—Research and Applications*, Vol. 691, Materials Research Society, Warrendale, PA, 2002, pp. 49–54.
- [10] Anno, H., Nagao, J., and Matsubara, K., "Electronic and Thermoelectric Properties of $\text{Yb}_y\text{Fe}_{4-x}\text{Ni}_x\text{Sb}_{12}$ Filled Skutterudites," *Proceedings of the 21th International Conference on Thermoelectrics*, Inst. of Electrical and Electronics Engineers, Piscataway, NJ, 2002, pp. 56–59.
- [11] Sales, B. C., Mandrus, D., and Williams, R. K., "Filled Skutterudite Antimonides: A New Class of Thermoelectric Materials," *Science*, Vol. 272, No. 5266, 1996, pp. 1325–1328. doi:10.1126/science.272.5266.1325
- [12] Mahan, G., Sales, B., and Sharp, J., "Thermoelectric Materials: New Approaches to an Old Problem," *Physics Today*, Vol. 50, No. 3, 1997, pp. 42–47.
- [13] Sales, B. C., Mandrus, D., Chakoumakos, B. C., Keppens, V., and Thompson, J. R., "Filled Skutterudite Antimonides: Electron Crystals and Phonon Glasses," *Physical Review B: Condensed Matter and Materials Physics*, Vol. 56, No. 23, 1997, pp. 15081–15089. doi:10.1103/PhysRevB.56.15081
- [14] Yang, L., Wu, J. S., and Zhang, L. T., "Thermoelectric Properties of Some Skutterudite Compounds with Different Grain Size," *Journal of Alloys and Compounds*, Vol. 375, Nos. 1–2, 2004, pp. 114–119. doi:10.1016/j.jallcom.2003.12.032

A. Gupta
Associate Editor